Pressure-Induced Structural Change of Liquid Silicon

Nobumasa Funamori
Department of Earth and Planetary Science, University of Tokyo, Tokyo 113-0033, Japan

Kazuhiko Tsuji
Department of Physics, Keio University, Yokohama 223-8522, Japan
(Received 21 November 2001; published 11 June 2002)

High-pressure and high-temperature x-ray diffraction measurements indicate that liquid silicon contracts with increasing pressure without significant changes in the local structure up to 8 GPa and then transforms to a denser structure between 8 and 14 GPa. In spite of volume contraction, the nearest-neighbor interatomic distance expands by about 1.6% within this pressure interval, accompanied by an anomalous increase in the coordination number. These findings reveal that the drastic pressure-induced structural change can take place in three-dimensional-network liquids with rather isotropic bonding.

DOI: 10.1103/PhysRevLett.88.255508 PACS numbers: 62.50.+p, 61.10.–i, 61.25.–f

Liquid silicon (l-Si) has attracted considerable attention because of its residual covalency [1] and the possibility of pressure- and/or temperature-induced polymorphic phase transitions [2,3], as well as the relevance to the crystal-growth process in the semiconductor industry. Numerous experimental [3–6] and theoretical [1,7] studies have suggested that the local structure of l-Si at ambient pressure is somewhat similar to high-pressure forms of crystalline Si (c-Si). In c-Si at room temperature, the semiconducting diamond structure contracts uniformly with pressure and transforms to the metallic white-tin structure at 12 GPa [8] and then to the metallic simple-hexagonal structure at 16 GPa [9]. However, the compression behavior of l-Si can be quite different from that of c-Si, as liquid structures are free from periodicity and are in general allowed to have plural local structures to minimize free energy. Indeed, according to the conventional two-species model [10], l-Si might consist of a mixture of diamond-type and white-tin-type structures and the ratio of the latter might increase with pressure. These motivate us to study the structure of l-Si at high pressures. Besides, the compression behavior of l-Si is important to discuss the compression mechanisms of liquids in terms of bonding. We have so far measured the compression behavior of simple liquids such as liquid alkali metals [11], in which constituent atoms are bonded with conduction s electrons, and of molecular and low-dimensional-network liquids such as liquid chalcogens [12,13] and liquid halogens [14], covalently bonded with p electrons. The measurements on l-Si provide the information on three-dimensional-network liquids, covalently bonded with hybrid s and p electrons. In this Letter, we report on the pressure-induced structural change of l-Si. Synchrotron x-ray diffraction measurements were made at 4, 8, 14, and 23 GPa at temperatures about 50 K above the melting point of each pressure [15], using recently developed experimental techniques [13]. The static structure factor $S(Q)$ and pair distribution function $g(r)$ of l-Si at high pressures [16] are shown in Figs. 1 and 2, and detailed structural information is summarized in Table I. Experimental and analytical procedures are described in detail elsewhere [13].

Significant changes in the local structure of l-Si occur between 8 and 14 GPa. The most obvious change can be observed in the first peak and its hump of $S(Q)$; i.e., the first peak shows an increase in intensity, while its hump shows a decrease (Fig. 1). To demonstrate the change in intensities, $S(Q_1)$ and $S(Q_h)$ are plotted as functions of pressure in Fig. 3. Here, Q_1 is the position of the first peak, and Q_h is the position of the hump and is just assumed to be $1.3Q_1$ to avoid the ambiguity in the determination of Q_h. As a result of the intensity change, the $S(Q_h)/S(Q_1)$ ratio, which is a measure of the variation of the shape of $S(Q)$, decreases significantly between 8 and 14 GPa (Table I). Besides, while the Q_1 increases monotonically with pressure, the second-peak position Q_2 decreases between 8 and 14 GPa, resulting in a decrease in Q_2/Q_1 (Table I).

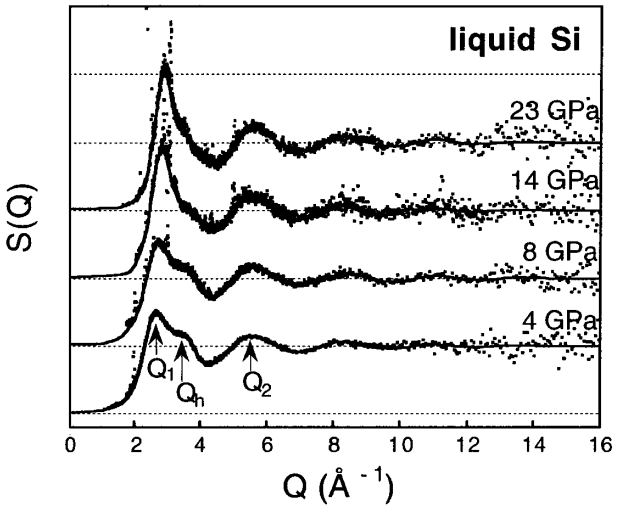

FIG. 1. The $S(Q)$ of l-Si measured at high pressures. Sharp peaks are diffraction lines of the sample container. Horizontal lines are drawn every one unit of $S(Q)$.

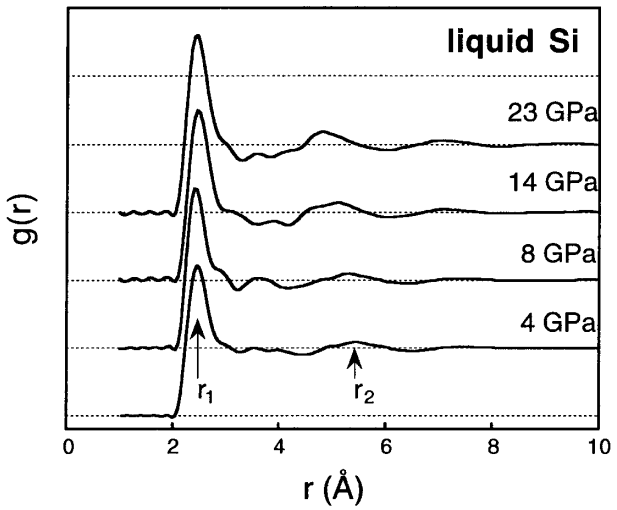

FIG. 2. The $g(r)$ of l-Si obtained by the Fourier transform of the $S(Q)$ shown in Fig. 1. Horizontal lines are drawn every one unit of $g(r)$.

The changes can be observed also in $g(r)$. The trough of $g(r)$ between the first and the second peak, which is obscure at 4 and 8 GPa, becomes significant above 14 GPa (Fig. 2). Furthermore, although the second-peak position r_2 decreases monotonically with pressure (Fig. 2), the first peak position r_1, i.e., the nearest-neighbor interatomic distance, increases against the compression between 8 and 14 GPa (Figs. 2 and 4, Table I). This strongly suggests that the structural change is accompanied by the increase in coordination number CN. Indeed, the CN, defined as the number of atoms at $r \leq r_c = 3.1$ Å, where r_c is a cutoff distance, shows an anomalous increase between 8 and 14 GPa [17] (Table I). Here, we adopt the definition of CN commonly used in theoretical work on l-Si at ambient pressure [1,7].

The local structure of l-Si at 4 and 8 GPa is quite similar to that at ambient pressure, as evident from the following comparison with experimental data at ambient pressure [3–6]. The large hump of $S(Q)$, which is the most characteristic feature at 4 and 8 GPa (Fig. 1), can be observed also at ambient pressure. The trough of $g(r)$ is obscure at ambient pressure, as well as at 4 and 8 GPa (Fig. 2). The $S(Q_h)/S(Q_1)$ at 4 and 8 GPa (Table I) is within the scatter of the data at ambient pressure, 0.74–0.85. Similarly, the Q_1, Q_2, and r_1 extrapolated to ambient pressure based on 4- and 8-GPa data are within the scatter (Table I). The relatively large scatter of the literature data may be due to the structural anomalies near the melting point at ambient pressure [3] and/or differences in experimental and analytical procedures. Moreover, the correction on r_c assuming the uniform contraction, i.e., r_c/r_1 is constant (cf. r_c is constant in Table I), gives $CN = 6.5$ for both 4- and 8-GPa data [17], which agrees very well with theoretical calculations at ambient pressure [1,7].

Structural information of other group-IV liquids, liquid germanium (l-Ge) [18] and liquid tin (l-Sn) [4], at ambient pressure is useful to interpret the present high-pressure data on l-Si [19]. The overall shape of $S(Q)$ of l-Si below 8 GPa is similar to that of l-Ge with $S(Q_h)/S(Q_1) \approx 0.8$, while the shape above 14 GPa is similar to that of l-Sn with $S(Q_h)/S(Q_1) \approx 0.4$. The trough of $g(r)$ is not clear in l-Si below 8 GPa, as well as in l-Ge but is clear in l-Si above 14 GPa as well as in l-Sn. Similarly, the Q_2/Q_1 of l-Si below 8 GPa is close to that of l-Ge, while the Q_2/Q_1 above 14 GPa is close to that of l-Sn (Table I). The r_1 of l- and c-Si are plotted as a function of pressure in Fig. 4. Here, the r_1 of the diamond-type, the white-tin-type, and the simple-hexagonal-type crystal is defined as the average distance of 4, 6, and 8 (i.e., CN for each structure) nearest-neighbor atoms, respectively. The r_1 of l-Si at 4 and 8 GPa and of l-Ge is longer than that of the diamond-type crystals and is shorter than that of the white-tin-type, whereas the r_1 at 14 GPa and of l-Sn is slightly longer than that of the white-tin-type crystals (Fig. 4, Table I). The r_1 at 23 GPa gets slightly closer to that of the simple-hexagonal-type crystal than at 14 GPa (Fig. 4). These observations suggest that l-Si contracts with pressure almost uniformly up to at least 8 GPa by reducing the bond length and then transforms to higher-CN structures via l-Sn-type structure. As c-Sn has

TABLE I. Structural information of l-Si at high pressures.

Material	P (GPa)	Q_1 (Å^{-1})	Q_2 (Å^{-1})	Q_2/Q_1	$S(Q_1)$	$S(Q_h)$[a]	$S(Q_h)/S(Q_1)$	r_1 (Å)	CN[b]	c-r_1 (Å)[c]	c-structure	Reference
Si	0	2.49	5.53	2.22				2.47		2.35	Diamond	[4]
Si	0	2.72	5.62	2.07				2.50		2.35	Diamond	[6]
Si	4	2.67	5.56	2.08	1.49	1.17	0.79	2.46	6.8	2.33	Diamond	This work
Si	8	2.72	5.61	2.06	1.55	1.16	0.75	2.42	7.1	2.30	Diamond	This work
Si	14	2.82	5.53	1.96	1.90	0.98	0.52	2.46	8.5	2.55	Simple-hexagonal	This work
Si	23	2.88	5.53	1.92	2.10	0.96	0.46	2.43	9.2	2.50	Simple-hexagonal	This work
Ge	0	2.48	5.10	2.06				2.66		2.45	Diamond	[18]
Sn	0	2.21	4.43	1.96				3.13[d]		3.07	White-tin	[4]

[a]Assumed as $Q_h = 1.3Q_1$.
[b]Defined as the number of atoms at $r \leq r_c = 3.1$ Å.
[c]Defined as the average distance of four, six, and eight neighbor atoms for the diamond, the white-tin, and the simple-hexagonal structure, respectively.
[d]Obtained from the tabulated $g(r)$ data of l-Sn.

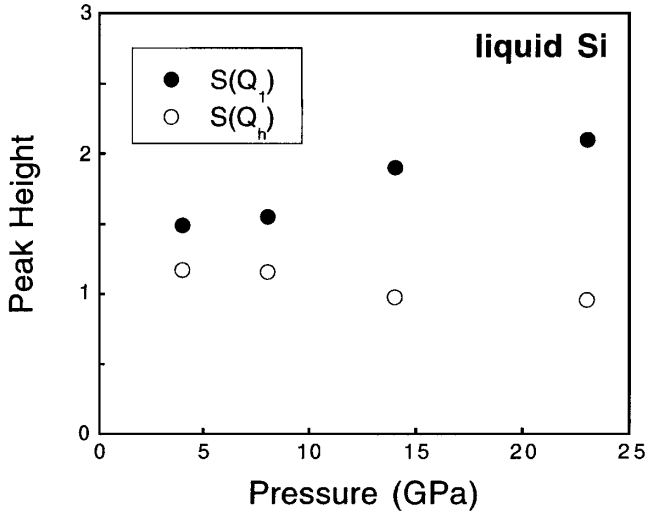

FIG. 3. Pressure dependence of the peak height of $S(Q_1)$ and $S(Q_h)$, demonstrating the drastic change between 8 and 14 GPa.

the white-tin structure and the density difference between c- and l-Sn is small [4], l-Sn-type structure is most likely related to the white-tin structure. Therefore, we believe that l-Si has an intermediate local structure between the diamond-type and the white-tin-type structure at pressures at least up to 8 GPa.

The occurrence of an intermediate local structure seems to be reasonable. The diamond structure, with perfect sp^3 hybrid bonding, most likely has a low entropy, and is therefore unfavorable at high temperatures where the contribution of the $-TS$ term to free energy is large (where T and S are temperature and entropy, respectively). On the other hand, as the potential energy of the white-tin structure is high, this structure is stable only at high pressures where the contribution of the PV term is large (where P and V are pressure and volume, respectively). Therefore, both the diamond-type and the white-tin-type local structure may be unstable at relatively low pressures below 8 GPa at high temperatures. Moreover, the difference in potential energy between the diamond and the white-tin structure is quite large as evident from theoretical calculations [20,21], and, indeed, several intermediate metastable forms of c-Si have been found so far [20,22]. The occurrence of an intermediate structure in l-Si may be supported by the observations that the density increase is about 10% upon the melting of the diamond structure at ambient pressure [4], while it is more than 20% at the transition from the diamond to the white-tin structure in c-Si at 12 GPa [8]. The white-tin structure can be regarded as a distorted-diamond structure with a tetragonal axial ratio of $c/a \approx 0.5$. Therefore, the distorted-diamond structure with an intermediate c/a ratio between 0.5 and 1, including the topologically disordered white-tin structure, which has been proposed by the reverse Monte Carlo simulations [18,23] and is consistent with the structural information from theoretical calculations [1,7], may be a candidate structure. The linear decrease of melting temperature with pressure [24] is in good accord with the inference that the intermediate structure contracts with pressure almost uniformly. The conventional two-species model [10] seems to be unsuitable for l-Si.

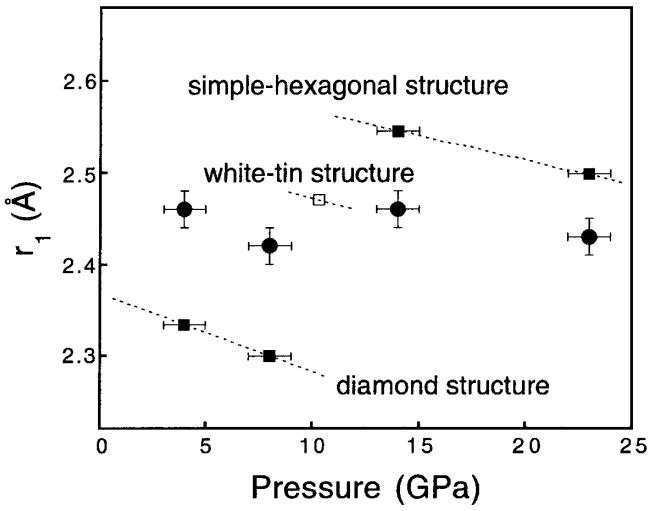

FIG. 4. Pressure dependence of the r_1 or l- and c-Si. The data for l-Si, measured at temperatures about 50 K above the melting point of each pressure, are plotted as solid circles. Uncertainties in pressure and the r_1 of l-Si are estimated to be within ± 1 GPa and ± 0.02 Å, respectively [13]. The data for the diamond and simple-hexagonal structures were measured at temperatures about 100 K below the melting point. The datum for the white-tin structure at room temperature is taken from literature [27].

The compression behavior of l-Si shows marked contrast with that of the liquids having different bonding mechanisms such as alkali metals [11], chalcogens [12,13], and halogens [14]. The liquid alkali metals, bonded with conduction s electrons (spherical orbital), are classified to simple liquids described by the conventional hard-sphere model [25]. The liquid alkali metals contract uniformly with pressure by reducing the effective radius of the hard sphere due to the screening effects by electrons. The liquid chalcogens and halogens, covalently bonded with p electrons (three orthogonal orbitals), are classified to molecular or low-dimensional-network liquids having a significantly distorted simple-cubic structure. The distortion is due to the formation of strong covalent bonds and the resultant long and short interatomic distances. The long interatomic distances contract with pressure selectively because of the weak coupling, resulting in electronic-charge redistribution and the weakening of the covalent bonds. Therefore, the distortion of the structure (microscopic anisotropy) is reduced by applied pressure. In this case, the r_1 expands and the first peak of $g(r)$ broadens with pressure. On the other hand, l-Si, covalently bonded with hybrid s and p electrons, can be classified to three-dimensional-network liquids and is rather isotropic even at ambient pressure. Our data suggest that l-Si contracts almost uniformly with pressure up to at least 8 GPa without significant changes in bonding and then transforms to a dense structure by

recoupling the bonding. The compression does not cause the broadening of the first peak of $g(r)$ at least up to 23 GPa (Fig. 2).

As evident from the above discussion, compression behavior of liquids largely depends on the nature of bonding. Liquids show a wide variety of structural changes, including a first-order transition from molecular to polymeric liquids recently found in liquid phosphorus (l-P) at around 1 GPa [26] by similar x-ray diffraction techniques. The present study provides the experimental evidence of the significant structural change, accompanied by increases in r_1 and CN, in three-dimensional-network liquids.

We are grateful to K. Funakoshi, W. Utsumi, and T. Kikegawa for experimental support. Synchrotron x-ray diffraction experiments were carried out at SPring-8 and PF using SPEED-1500 and MAX-III systems. This work is in part supported by Itoh Science Foundation, The Kurata Foundation, Grant-in-Aid for Exploratory Research (Japanese government), and Grant-in-Aid for Scientific Research (Japanese government).

[1] I. Stich, R. Car, and M. Parrinello, Phys. Rev. Lett. **63**, 2240 (1989).
[2] P. H. Poole *et al.,* Science **275**, 322 (1997); S. K. Deb *et al.,* Nature (London) **414**, 528 (2001).
[3] S. Ansell *et al.,* J. Phys. Condens. Matter **10**, L73 (1998), and references therein.
[4] Y. Waseda, in *The Structure of Non-Crystalline Materials* (McGraw-Hill, New York, 1980).
[5] Y. Waseda and K. Suzuki, Z. Phys. B **20**, 339 (1975); J. P. Gabathuler and S. Steeb, Z. Naturforsch. **34A**, 1314 (1979); Y. Waseda *et al.,* Jpn. J. Appl. Phys. **34**, 4124 (1995).
[6] S. Takeda, Jpn. J. Appl. Phys. **34**, 4889 (1995).
[7] For example, E. Kim and Y. H. Lee, Phys. Rev. B **49**, 1743 (1994); I. Stich, M. Parrinello, and J. M. Holender, Phys. Rev. Lett. **76**, 2077 (1996); M. Ishimaru *et al.,* Phys. Rev. B **54**, 4638 (1996); C. S. Liu *et al., ibid.* **60**, 3194 (1999); N. Jakse, Y. Kadiri, and J. L. Bretonnet, *ibid.* **61**, 14 287 (2000).
[8] J. C. Jamieson, Science **139**, 762 (1963).
[9] H. Olijnyk, S. K. Sikka, and W. B. Holzapfel, Phys. Lett. **103A**, 137 (1984); J. Z. Hu and I. L. Spain, Solid State Commun. **51**, 263 (1984).
[10] E. Rapoport, J. Chem. Phys. **46**, 2891 (1967).
[11] K. Tsuji *et al.,* J. Non-Cryst. Solids **205–207**, 295 (1996).
[12] K. Tsuji *et al.,* Rev. Sci. Instrum. **60**, 2425 (1989); K. Tsuji, J. Non-Cryst. Solids **117–118**, 27 (1990).
[13] N. Funamori and K. Tsuji, Phys. Rev. B **65**, 014105 (2001).
[14] T. Mori, K. Tsuji, and N. Funamori (to be published).
[15] Energy-dispersive x-ray diffraction measurements were carried out at the SPring-8 and PF synchrotron facilities in Japan using the SPEED-1500 (at 8, 14, and 23 GPa) and MAX-III (at 4 GPa) systems, respectively. Temperature was estimated from the melting curve of Si [24], assuming proportionality between temperature and supplied electric power for heating. Pressure was determined by the sodium chloride (NaCl) internal-pressure-standard method [D. L. Decker, J. Appl. Phys. **42**, 3239 (1971)].
[16] To obtain $g(r)$, number density is tentatively assumed to be 0.058, 0.060, 0.067, and 0.071 atoms/Å^3 at 4, 8, 14, and 23 GPa, respectively, based on available thermoelastic data [4,9,24].
[17] Discussion on CN at 14 and 23 GPa may not be robust because of uncertainty in number density. However, the anomalous increase in CN between 8 and 14 GPa is too large to be explained as the artificial due to the uncertainty. Meanwhile, number density is rather accurate and so is CN at 4 and 8 GPa.
[18] V. Petkov *et al.,* J. Non-Cryst. Solids **168**, 97 (1994).
[19] Structural information of amorphous Si (a-Si) [e.g., J. Fortner and J. S. Lannin, Phys. Rev. B **39**, 5527 (1989)] is also useful. The local structure of a-Si is considered to be related to the diamond structure. The overall shape of $S(Q)$ of a-Si is completely different from that of l-Si at any pressures and the r_1 of a-Si is close to that of the diamond-type crystal.
[20] R. O. Piltz *et al.,* Phys. Rev. B **52**, 4072 (1995).
[21] For example, M. T. Yin and M. L. Cohen, Phys. Rev. Lett. **45**, 1004 (1980); B. G. Pfrommer *et al.,* Phys. Rev. B **56**, 6662 (1997).
[22] R. H. Wentorf, Jr. and J. S. Kasper, Science **139**, 338 (1963); Y. Zhao *et al.,* Solid State Commun. **59**, 679 (1984).
[23] V. Petkov and G. Yunchov, J. Phys. Condens. Matter **6**, 10 885 (1994).
[24] P. F. Bundy, J. Chem. Phys. **41**, 3809 (1964).
[25] N. W. Ashcroft and J. Lekner, Phys. Rev. **145**, 83 (1966).
[26] Y. Katayama *et al.,* Nature (London) **403**, 170 (2000).
[27] M. I. McMahon and R. J. Nelmes, Phys. Rev. B **47**, 8337 (1993).